The Journal of Physiology

The molecular mechanism of synaptic activity-induced astrocytic volume transient

Junsung Woo[1,*], Minwoo Wendy Jang[2,3,*], Jaekwang Lee[1], Wuhyun Koh[3,4], Katsuhiko Mikoshiba[5] and C. Justin Lee[1,2,3,4]

[1]*Center for Glia-Neuron Interaction, Korea Institute of Science and Technology (KIST), Seoul 02792, Republic of Korea*
[2]*KU-KIST Graduate School of Converging Science and Technology, Korea University, Seoul 02841, Republic of Korea*
[3]*Center for Cognition and Sociality, Institute for Basic Science (IBS), Daejeon 34126, Republic of Korea*
[4]*Department of Neuroscience, Division of Bio-Medical Science & Technology, KIST School, Korea University of Science and Technology (UST), Seoul 02792, Republic of Korea*
[5]*Laboratory for Developmental Biology, RIKEN Brain Science Institute, Hirosawa 2-1, Wako, Saitama 351-0198, Japan*

Edited by: David Wyllie & Vincenzo Marra

Key points

- Neuronal activity causes astrocytic volume change via K^+ uptake through TREK-1 containing two-pore domain potassium channels.
- The volume transient is terminated by Cl^- efflux through the Ca^{2+}-activated anion channel BEST1.
- The source of the Ca^{2+} required to open BEST1 appears to be the stretch-activated TRPA1 channel.
- Intense neuronal activity is synaptically coupled with a physical change in astrocytes via volume transients.

Abstract The brain volume changes dynamically and transiently upon intense neuronal activity through a tight regulation of ion concentrations and water movement across the plasma membrane of astrocytes. We have recently demonstrated that an intense neuronal activity and subsequent astrocytic AQP4-dependent volume transient are critical for synaptic plasticity and memory. We have also pharmacologically demonstrated a functional coupling between synaptic activity and the astrocytic volume transient. However, the precise molecular mechanisms of how intense neuronal activity and the astrocytic volume transient are coupled remain unclear. Here we utilized an intrinsic optical signal imaging technique combined with fluorescence imaging using ion sensitive dyes and molecular probes and electrophysiology to investigate the detailed molecular mechanisms in genetically modified mice. We report that a brief synaptic activity induced by a train stimulation (20 Hz, 1 s) causes a prolonged astrocytic volume transient (80 s)

Junsung Woo was a postdoc fellow in the Center for Glia-Neuron Interaction at Korea Institute of Science and Technology and is currently a postdoc fellow in the Center for Cell and Gene Therapy at Baylor College of Medicine. **Minwoo Wendy Jang** is a PhD candidate of KU-KIST Graduate School of Converging Science and Technology, Korea University in the laboratory of Dr C. Justin Lee.

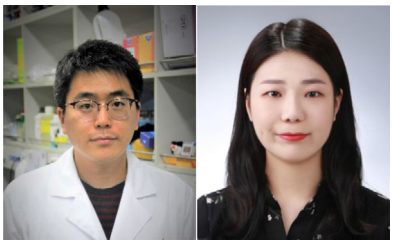

*J. Woo and M. W. Jang contributed equally to this work.

DOI: 10.1113/JP279741

via K^+ uptake through TREK-1 containing two-pore domain potassium (K2P) channels, but not Kir4.1 or NKCC1. This volume change is terminated by Cl^- efflux through the Ca^{2+}-activated anion channel BEST1, but not the volume-regulated anion channel TTYH. The source of the Ca^{2+} required to open BEST1 appears to be the stretch-activated TRPA1 channel in astrocytes, but not IP_3R2. In summary, our study identifies several important astrocytic ion channels (AQP4, TREK-1, BEST1, TRPA1) as the key molecules leading to the neuronal activity-dependent volume transient in astrocytes. Our findings reveal new molecular and cellular mechanisms for the synaptic coupling of intense neuronal activity with a physical change in astrocytes via volume transients.

(Received 20 March 2020; accepted after revision 20 July 2020; first published online 24 July 2020)
Corresponding author C. Justin Lee: Center for Cognition and Sociality, Institute for Basic Science (IBS), 55, Expo-ro, Yuseong-gu, Daejeon 34126, Republic of Korea. Email: cjl@ibs.re.kr

Introduction

Astrocytes are the most abundant cell type in the brain and are known to play many critical roles under physiological as well as pathological conditions. In an active role, astrocytes modulate synaptic transmission and plasticity by releasing various gliotransmitters upon Ca^{2+} rise (Verkhratsky & Kettenmann, 1996; Araque *et al.* 1999; Lee *et al.* 2007; Thrane *et al.* 2011; Woo *et al.* 2012; Park *et al.* 2015; Bazargani & Attwell, 2016; Nam *et al.* 2019). In a supportive role, astrocytes maintain appropriate ionic concentrations in extracellular space, for example, by taking up potassium ions (K^+) during and after intense synaptic transmission (Simard & Nedergaard, 2004; Lambert *et al.* 2008; Dallerac *et al.* 2013). During this process, the water molecules initially follow the movement of K^+ via the astrocyte-specific water channel, aquaporin-4 (AQP4), resulting in a transient volume increase in the astrocyte (Simard & Nedergaard, 2004; Andrew *et al.* 2007; Kitaura *et al.* 2009; Nagelhus & Ottersen, 2013; Woo *et al.* 2018, 2019). Then the astrocytic volume returns to normal by extruding chloride ions (Cl^-) and osmolytes, possibly via anion channels (Abdullaev *et al.* 2006; Mulligan & MacVicar, 2006; Okada *et al.* 2009; Woo *et al.* 2019), followed by a subsequent water efflux through AQP4.

Regarding the astrocytic K^+ uptake mechanism, many studies have revealed that the extracellular K^+ originates from the neuronal postsynaptic glutamate receptor channels that open and release during excitatory synaptic transmission (MacVicar & Hochman, 1991; Djukic *et al.* 2007; Cheung *et al.* 2015; Woo *et al.* 2019). However, the exact molecular identity of the channel or transporter responsible for the K^+ uptake in astrocytes has not been determined. Various potential molecular candidates have been proposed in the past; Kir4.1 (inwardly rectifying K^+ channel), NKCC1 (Na^+, K^+, $2Cl^-$ cotransporter), Na^+/K^+-ATPase, and K2P (two-pore domain K^+ channels) (MacVicar *et al.* 2002; Su *et al.* 2002; Djukic *et al.* 2007; Pasler *et al.* 2007; Macaulay & Zeuthen, 2012). Likewise, the molecular identity of the anion channel which is responsible for the efflux of Cl^- and osmolytes has not been determined, though it has been proposed that the volume regulated anion channel (VRAC) might be involved (Mulligan & MacVicar, 2006; Okada *et al.* 2009; Han *et al.* 2019; Woo *et al.* 2019; Yang *et al.* 2019).

Intriguingly, the astrocytic volume transient appears to be linked to synaptic plasticity and memory. Many previous studies, including ours, have revealed that the mice lacking *Aqp4* consistently show impaired synaptic plasticity and memory (Skucas *et al.* 2011; Fan *et al.* 2013; Szu & Binder, 2016; Woo *et al.* 2018). However, it has been difficult to understand the nature of the neuronal activity-induced transient volume change in astrocytes and how it influences synaptic transmission, synaptic plasticity, and memory. This is perhaps due to the lack of mechanistic insights into the astrocytic volume regulation that leads to water movement. Therefore, the exact mechanism underlying AQP4-mediated plasticity and memory still remains elusive.

To address these topics, we have optimized and utilized the intrinsic optical signal (IOS) imaging technique (MacVicar & Hochman, 1991; Holthoff & Witte, 1996; MacVicar *et al.* 2002; Woo *et al.* 2018, 2019) to indirectly monitor transient volume changes in real-time from hippocampal slices of various genetically modified mice by detecting the light transmittance through a brain slice during and after intense neuronal activity (Fig. 1*A* and *B*) . We defined the neuronal activity-induced volume transient as the volume change in astrocytes that occurs within a minute of intense neuronal activity (MacVicar & Hochman, 1991; Holthoff & Witte, 1996; MacVicar *et al.* 2002; Woo *et al.* 2019). Using IOS imaging, we delineate the detailed molecular mechanism of the astrocytic volume transient and further demonstrate how intense neuronal activity is synaptically coupled with a physical change in astrocytes via volume transients.

Methods

Ethical approval

All experimental procedures were conducted according to protocols approved by the directives of the Institutional Animal Care and Use Committee (IACUC) of Korea Institute of Science and Technology (KIST, Seoul, Korea, No. 2016–051) and Institute for Basic Science (IBS, Daejeon, Korea, No. IBS 18-11). Breeding and housing of the animals were conducted in the departmental animal facility, with free access to water and rodent laboratory chow. The animal facility was specific pathogen free, with a 12 h-light/12 h-dark cycle, and mice were 3–5 per cage. Experimental protocols were designed to minimize suffering and the number of animals used in the study. The authors understand the ethical principles under which *The Journal of Physiology* operates and confirm that this work meets the standards of *The Journal*'s animal ethics checklist.

Animals

Adult (7∼10 weeks) male and female wildtype (C57BL/6, Jackson Laboratories, RRID: IMSR_JAX:000664), Best1 KO (Balb/C, Marmorstein *et al.* 2006, RRID: MGI:3797408), TRPA1 KO (129, Jackson Laboratory, RRID: IMSR_JAX:006401), NKCC1 KO (B6/129, Jackson Laboratories, RRID:MGI:2174739), IP_3R2 KO (C57BL/6, Futatsugi *et al.* 2005, kindly provided by Dr. Katsuhiko Mikoshiba), and their wild littermate mice were used. A 1–5% isoflurane inhalation protocol was used for anaesthesia. Isoflurane was delivered in the induction chamber with an oxygen source and a precision vaporizer, and equipped with a gas scavenging system. Aanaesthetic depth was monitored by toe pinch. All experimental animals were killed under anaesthesia, in an unconscious state.

Slice preparation

Hippocampal slices were prepared as previously described (Woo *et al.* 2019). Briefly, mice were kept under 2–4% isoflurane inhalation for anaesthesia. Mice heads were decapacitated in the anaesthetized state. Then, brains were extracted rapidly and placed in ice-cold, oxygenated (95% O_2 and 5% CO_2) high Mg^{2+} dissection buffer containing (in mM) 130 NaCl, 24 $NaHCO_3$, 3.5 KCl, 1.25 NaH_2PO_4, 1 $CaCl_2$, 3 $MgCl_2$, and 10 glucose (pH

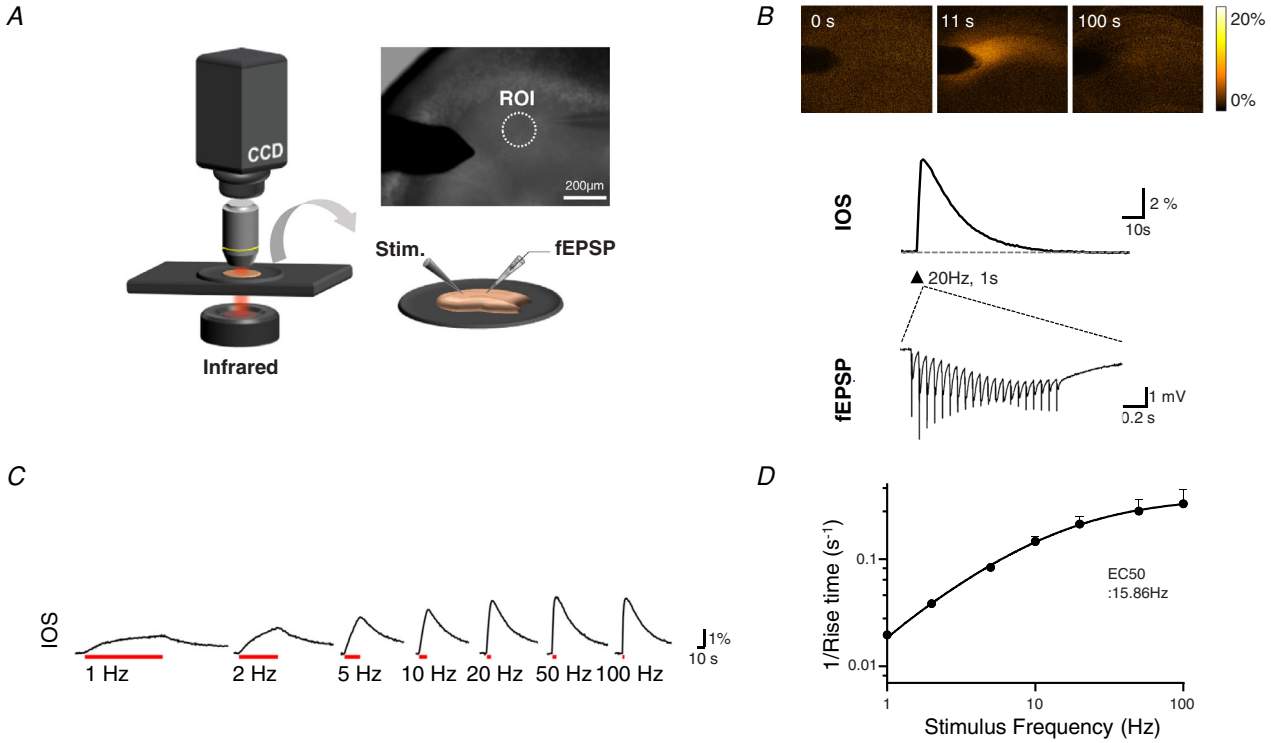

Figure 1. Transient volume change is highly dependent on the strength of synaptic activity
A, schematic diagram. Simultaneous recording of IOS and field EPSP (fEPSP) in the stratum radiatum region of the mouse hippocampus after stimulating the Schaffer collateral pathway. *B*, representative traces of IOS and fEPSP upon intense electrical stimulation of Schaffer collateral fibres for 1 s at 20 Hz. *C*, representative IOS traces recorded at different stimulus frequencies but the same pulse number. *D*, normalized IOS inverse rise time with increasing stimulus frequencies. Non-linear fitting with a three parameter dose-response curve equation was used: $Y = \text{Bottom} + X \times (\text{Top} - \text{Bottom})/(EC_{50} + X)$. The R^2 value is 0.9992.

7.4). Transverse slices containing hippocampus were obtained at a thickness of 300 μm using a D.S.K Linear Slicer pro7 (Dosaka EM Co., Ltd, Japan). Slices were recovered for at least 1 h before recording in high Mg^{2+} dissection buffer at room temperature. After 1 h, the Mg^{2+} dissection buffer was changed to oxygenated aCSF containing (mM) 130 NaCl, 24 $NaHCO_3$, 3.5 KCl, 1.25 NaH_2PO_4, 1.5 $CaCl_2$, 1.5 $MgCl_2$, and 10 glucose (pH 7.4) for additional recovery or IOS, field recording experiments.

Intrinsic optical signal imaging

Submerged slices were transilluminated using a controlled infrared (IR) light source with optical filter (775 nm wavelength, Omega Filters), and images were taken using a microscope (Olympus, BX50WI) equipped with a digital CCD camera (Hamamatsu, ORCA-R2). We imaged the stratum radiatum of the hippocampal CA1 region. A series of 80 images was acquired per second after 20 Hz, 1 s electrical stimulation. The relative change of transmittance ($\Delta T/T$) was normalized to baseline (average of 5 images). Decay of the intrinsic optical signal (IOS) was measured by averaging the last 10 s of the response after dividing responses by the peak response. Imaging Workbench software (INDEC BioSystems) was used for image acquisition and analysis.

Electrophysiology

Whole-cell patch recordings were obtained from SR101-loaded astrocytes in hippocampal stratum radiatum in current clamp configuration using a Multiclamp 700B amplifier (Axon Instruments, Union City, NJ, USA) and a borosilicate patch pipette of 5-8 MΩ resistance. Recording electrodes were filled with internal solution containing (mM) 126 potassium gluconate, 5 HEPES, 0.5 $MgCl_2$ and 10 BAPTA (pH adjusted to 7.3 with KOH) and advanced through the tissue under positive pressure. The stimulating electrode was positioned 400 μm away from the patch-clamped astrocyte. Records were filtered at 2 kHz and digitized at 10 kHz using a Digidata 1322A (Axon Instruments). Field EPSP recording was performed as described previously (Woo *et al.* 2019). In brief, field EPSP in CA1 stratum radiatum was evoked by Schaffer-collateral stimulation with a concentric bipolar stimulation electrode (FHC, Bowdoin, ME, USA). Recording electrodes with a resistance of 1-3 MΩ were prepared and filled with aCSF. The amplitude of field EPSP was quantified for further analysis. Recording was performed using a Multiclamp 700B amplifier (Molecular Devices). Data were acquired and analysed with pClamp 10.2.

K^+ imaging

The movement of K^+ in astrocytes and neurons was assessed with the K^+-selective fluorescence indicator Asante Potassium Green 1 (APG-1) from TEFLabs. Astrocytes and neurons were identified by their morphology and electrical properties. SR-101 staining was used to characterize astrocytes. Cells were patched with a pipette solution composed of (in mM) 140 potassium gluconate, 10 HEPES, 7 NaCl, and 2 MgATP adjusted to pH 7.4 with CsOH containing APG-1 (40 μM). After a 15 min period, during which dye diffused into the cell, images of APG-1 fluorescence were acquired using a microscope equipped with a mercury lamp, and the dye was excited at 440 nm (540 nm emission). A series of 20 images was acquired per second after 20 Hz stimulation.

Cl^- imaging

For epifluorescence Cl^- imaging, astrocytes were patched with the Cl^--selective dye, 6-methoxy-*N*-ethylquinolinium iodide (MEQ, 5 mM, Invitrogen) in a pipette solution composed of (in mM) 140 potassium gluconate, 10 HEPES, 7 NaCl, and 2 MgATP adjusted to pH 7.4 with CsOH. Cl^- imaging was performed as previously described (Isomura *et al.* 2003). SR-101 staining was used to characterize astrocytes. The light from a mercury lamp was directed through a 335 nm excitation filter and deflected by a 360 nm dichroic beam splitter. Fluorescence emission was directed through a 440 nm filter and detected with a digital CCD camera. A series of 80 images was acquired per second after 20 Hz electrical stimulation. The relative change of transmittance was normalized to baseline (average of 20 images). Response was measured by averaging responses during the last 10 s.

Ca^{2+} imaging

For Ca^{2+} imaging experiments, slices were loaded with Fura-2 AM (10 μM, 1 h). Image intensities of 510 nm wavelength were taken at 340 nm and 380 nm excitation wavelengths using a CCD camera. Two resulting images were used for ratio calculations with Axon Imaging Workbench version 6.2 software (Axon Instruments). SR-101 staining was used for astrocyte characterization. A series of 60 images was acquired per second after electrical stimulation. The relative change was normalized to baseline (average of 20 images). For Ca^{2+} imaging using a Ca^{2+} sensor, AAV-GFAP104-jRGECO1a was injected unilaterally into the hippocampal CA1 region at rate of 0.1 μl/min (total 0.5 μl) with a 25 μl syringe using a syringe pump (KD Scientific, USA). The stereotaxic coordinates of the injection site were ML: 1.6 mm, AP: −1.8 mm and DV: −1.6 mm away from the bregma.

Virus injection and Cre activation for glia-specific gene rescue

Mice (7-8 weeks old) were anaesthetized by 3–5% isoflurane inhalation and placed into stereotaxic frames. The isoflurane concentration was lowered to 1–3% during surgical procedures, which were performed within 1 h for each mouse. pSicoR lentivirus containing target shRNA for *Trek-1*, *Kir4.1*, *Aqp4*, *Trpa1* and *Best1* or AAV-GFAP-GFP and AAV-GFAP-Cre virus was loaded into a micro dispenser (VWR, Radnor, PA, USA) and injected bilaterally into the hippocampal CA1 region at a rate of 0.3 μl/min (total 2 μl) with a 25 μl syringe using a syringe pump (KD Scientific, USA). In experiments using the triple combination of TTYH shRNA, we used either (pSicoR-*Ttyh1*-shRNA-GFP, pSicoR-*Ttyh2*-shRNA-mcherry and pSicoR-*Ttyh3*-shRNA-mcherry) or (pSicoR-scrambled-shRNA-GFP and pSicoR-scrambled-shRNA-mcherry). The stereotaxic coordinates of the injection site were 1.7 mm away from the bregma and the depth was 1.9 mm beneath the skull. Our glia-specific gene rescue strategy was based on flanking the target shRNA cassette with a pair of loxP sites, so that Cre-loxP recombination would cause excision of this cassette and inactivate the target shRNA (Ventura *et al.* 2004). By injecting this virus into a mouse line (hGFAP-CreERT2) that conditionally expresses Cre in glial cells only, we could selectively retain target gene expression in glial cells (Lee *et al.* 2010; Woo *et al.* 2012). Glial-specific activation of CreERT2 was initiated by intraperitoneal injection of tamoxifen. For Cre activation, 1 mg of tamoxifen (dissolved in sunflower oil), or sunflower oil solvent as a control, was intraperitoneally injected for 7 days prior to shRNA injection. All experiments were carried out under blind conditions.

Chemicals

D-AP5 (Cat. No. 0106), CNQX (Cat. No. 0190) and ORG24598 (Cat. No. 4447) were purchased from Tocris and 4-aminopyridine (A78403) was purchased from Sigma-Aldrich.

Statistical analysis

No statistical methods were used to pre-determine sample sizes but our sample sizes are similar to or larger than those generally employed in the fields. Collation of data was not randomized and was not done blindly, but experiments were repeated over a long study period (>2 years). No animals were excluded from the study. Data were presented as means ± S.D. and were analysed and graphed using Prism 7 (GraphPad, San Jose, CA, USA) and SigmaPlot (Systat Software, San Jose, CA, USA). When two groups were being compared, the significance of data were assessed by the two-tailed Student's *t* test. For comparison of multiple groups, one-way or two-way ANOVA was utilized. When there was an interaction between groups, the Bonferroni/Dunnett test or multiple *t* test was applied for *post hoc* analysis. In specific cases, one-way ANOVA with a Bonferroni/Dunnett/Tukey test was used to classify the homogenous subsets. In general, data distribution was assumed to be normal, but this was not formally tested.

Results

Volume transient is initiated by K^+ uptake via TREK-1 in astrocytes

The neuronal activity-dependent volume transient can be detected and visualized as an IOS with a fast rise (4–6 s) and slow decay (70–80 s) in light transmittance through CA1 hippocampal slices upon intense electrical stimulation of Schaffer collateral fibres for 1 s at 20 Hz (Fig. 1*A* and *B*), as previously described (MacVicar & Hochman, 1991; Andrew *et al.* 2007; Woo *et al.* 2019). The light scattering property of the brain slices changes as the water moves into or out of various cell types such as astrocytes, resulting in changes in light transmittance (MacVicar & Hochman, 1991; Holthoff & Witte, 1996; Kitaura *et al.* 2009; Woo *et al.* 2018). To determine the stimulation frequency-dependency of IOS, we stimulated CA1 stratum radiatum with different frequencies at the same pulse numbers (100 times) (Fig. 1*C*). The inverse of IOS rise time (s^{-1}) positively correlated with electrical stimulation frequency with half-maximal effective frequency (EC_{50}) at 15.86 Hz (Fig. 1*D*), indicating that transient volume change is highly dependent on the frequency of synaptic activity.

To replicate previous studies showing that the astrocytic water movement is required for the volume transient, we measured the IOS from the hippocampal slices of mice injected with a lentivirus carrying the *Aqp4* shRNA for 7 days leading to acute gene-silencing of *Aqp4* (Woo *et al.* 2018). We observed that the amplitude of the IOS, which is the measure of the increase of the volume transient, was almost completely abolished by *Aqp4* shRNA compared to control shRNA (Fig. 2*A* and *B*). On the other hand, there was no change in basal synaptic transmission between control and *Aqp4* shRNA infected groups (Fig. 2*C*). In order to examine the rescue effect of astrocytic *Aqp4*, we utilized the Cre-loxP system. *Aqp4* shRNA was cloned between 2 loxP sites, which can be flanked under GFAP promoter driven-Cre expression (Fig. 2*D*). We injected *Aqp4* shRNA with GFAP-GFP as a control group and with GFAP-Cre as an experimental group. The *Aqp4* shRNA resulted in a significant reduction in IOS signal in the control group which was significantly restored in the experimental group (Fig. 2*E* and *F*). These

findings confirmed that AQP4 indeed mediates astrocytic volume change. We also observed stimulus-dependent IOS responses in astrocytes expressing control shRNA and *Aqp4* shRNA. The control shRNA group showed a steep increase in IOS amplitude with gradually increasing stimulation frequency, compared to *Aqp4* shRNA group (Fig. 2*G*). Through these sets of experiments, we recapitulated our previous results that the *Aqp4* knockdown system does not alter synaptic activity and that astrocytic water movement through AQP4 is required for the astrocytic volume transient.

Volume changes in astrocytes, especially astrocytic swelling under pathological conditions, are known to trigger many cellular events in these cells (Verkhratsky & Kettenmann, 1996; Bazargani & Attwell, 2016), including an increase in cytosolic Ca^{2+}. Because astrocytes utilize Ca^{2+} increases in major signalling pathways (Verkhratsky & Kettenmann, 1996; Verkhratsky *et al.* 1998; Bazargani & Attwell, 2016), we first tested to see whether the volume transient is associated with Ca^{2+} signalling in astrocytes. We recorded IOS from hippocampal slices and Ca^{2+} imaging from individual astrocytes while increasing the stimulus frequency from 1 Hz to 100 Hz and maintaining the stimulus duration at 1 s. We found that amplitudes of the IOS and Ca^{2+} transients were increased to a similar degree with a similar EC_{50} frequency of 20.36 Hz for IOS

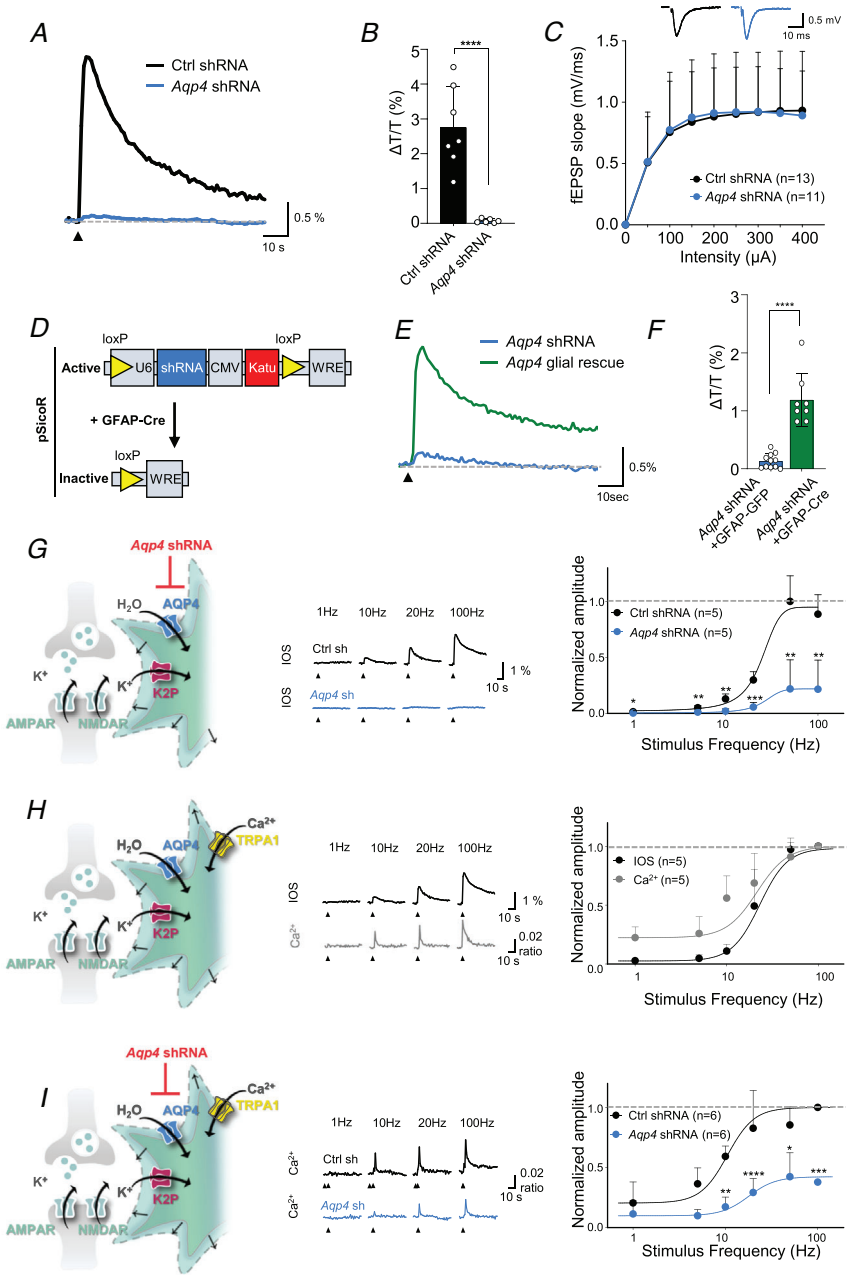

Figure 2. Synaptic activity dependent astrocytic volume and Ca^{2+} transient is mediated by AQP4 water channels
A, representative IOS traces from control and *Aqp4* shRNA expressing mice. *B*, summary bar graph of amplitude of IOS from *A* (Student's unpaired *t* test, $^{****}P < 0.0001$). *C*, input-output curve of fEPSP amplitude plotted *versus* stimulus intensity (μA). Inset: representative traces of fEPSP at 100 μA stimulation. *P* values were derived from two-way ANOVA with Bonferroni's *post hoc* multiple comparison test. N.S. $P > 0.05$. *D*, schematic diagram displaying *Aqp4* shRNA expression in the absence and presence of Cre expression. *E*, representative IOS traces from *Aqp4* shRNA expressing and *Aqp4* rescued mice. *F*, summary bar graph of amplitude of IOS from *E* (Student's unpaired *t* test, $^{****}P < 0.0001$). *G*, stimulus-dependent IOS responses in astrocytes expressing control shRNA and *Aqp4* shRNA. Middle: representative traces of IOS response (Student's unpaired *t* test $^{*}P < 0.05$, $^{**}P < 0.01$, $^{***}P < 0.001$). *H*, amplitude of IOS and Ca^{2+} response in astrocyte plotted *versus* stimulus intensity after normalization by peak response. Middle: representative traces of IOS and Ca^{2+} response. *I*, stimulus-dependent Ca^{2+} responses in astrocytes expressing control shRNA and *Aqp4* shRNA. Middle: representative traces of Ca^{2+} response (Student's unpaired *t* test $^{*}P < 0.05$, $^{**}P < 0.01$, $^{***}P < 0.001$, $^{****}P < 0.0001$).

and 19.86 Hz for Ca^{2+} transients (Fig. 2*H*). To directly test whether astrocytic Ca^{2+} transients are caused by the volume transient, we measured the stimulus-induced Ca^{2+} transients in astrocytes expressing *Aqp4* shRNA. The amplitude of Ca^{2+} transients was significantly reduced by about 65% by the *Aqp4* shRNA compared to control shRNA at 100 Hz, without altering the EC_{50} frequency (Fig. 2*I*). These data indicate that stimulus-induced neuronal activity leads to an astrocytic volume transient followed by an astrocytic Ca^{2+} transient.

We have previously reported that the quinine-sensitive K2P channel mediates astrocytic K^+ uptake and contributes to the main source of activity-dependent IOS (Woo *et al.* 2019). We also demonstrated that TREK-1 containing K2P channels mediate the passive conductance and GPCR-induced fast glutamate release in hippocampal astrocytes (Woo *et al.* 2012; Hwang *et al.* 2014). TREK-1-mediated glutamate release is involved in μ-opioid receptor-dependent hippocampal synaptic plasticity and conditioned place preference (Nam *et al.* 2019). Therefore, we tested for TREK-1 as an indicator that K2P channels are involved in the synaptic activity-dependent K^+ uptake and the volume transient. To determine whether the astrocytic TREK-1 is responsible for the volume change, we used a Cre-loxP-dependent conditional gene silencing system with a lentivirus containing the previously characterized *Trek-1* shRNA (Lee *et al.* 2010; Woo *et al.* 2012). In hGFAP-CreERT2 mice (tamoxifen-inducible human GFAP promoter-driven Cre transgenic mice) infected with *Trek-1* shRNA resulting in a general knockdown of the K2P channel; the amplitude of the IOS was significantly reduced compared to the control shRNA condition and the uninfected control (Fig. 3*A* and *B*). However, treatment of hGFAP-CreERT2 mice with tamoxifen before injection of *Trek-1* shRNA, which resulted in an astrocyte-specific gene rescue of *Trek-1*, fully restored the amplitude of the IOS to its control level (Fig. 3*A* and *B*). There was no change in basal synaptic transmission between the two virus-infected groups (Fig. 3*C*). These results indicate that the astrocytic TREK-1 containing K2P channel is responsible for the majority (about 70%) of the increase of volume transient.

To test whether the astrocytic K2P channel is directly responsible for the K^+ uptake, we measured K^+ movement in neurons and astrocytes during synaptic transmission by using a K^+ selective fluorescent dye, APG-1 (Bittner *et al.* 2013). As expected, we observed an efflux and an influx of K^+ in APG-1 loaded neurons and astrocytes, respectively, which were both blocked (about 80%) by postsynaptic glutamate receptor blockers, APV and CNQX (Fig. 3*D*–*F*). In *Trek-1* shRNA-expressing astrocytes, we observed an almost complete elimination of K^+ influx (Fig. 3*G* and *H*) and membrane depolarization (Fig. 3*I* and *J*) compared to control shRNA-expressing astrocytes, indicating that the TREK-1 containing K2P channel is responsible for K^+ uptake. To see whether K^+ uptake precedes the IOS, we compared the time course of K^+ uptake, IOS, and membrane depolarization of astrocytes. We found that both K^+ movement and membrane depolarization preceded IOS (time to peak: 1 s for membrane depolarization, 2 s for K^+ uptake, and 5 s for IOS) (Fig. 3*K* and *L*), which suggest that the volume transient is initiated by K^+ uptake via TREK-1 in astrocytes.

We next tested two other possible candidates, NKCC1 and Kir4.1, as targets for transient volume increase, using genetic knockout (KO) or knockdown models. We observed no change of IOS amplitude in wildtype (WT) littermates, hetero-types, and KO mice for NKCC1 (Fig. 4*A* and *B*). The next candidate, Kir4.1, has long been proposed as the molecular target for K^+ buffering in astrocytes (Djukic *et al.* 2007; Olsen & Sontheimer, 2008). To test the involvement of Kir4.1 in the volume transient, we utilized the previously developed specific shRNA for *Kir4.1* (Hwang *et al.* 2014). Contrary to expectations, we found no change of IOS amplitude between *Kir4.1* gene-silenced condition and control shRNA condition (Fig. 4*C* and *D*). These data suggest that the volume transient is not mediated by NKCC1 or Kir4.1. To test a possible involvement of Kir4.1 in K^+ uptake, we utilized APG-1 (Bittner *et al.* 2013) in *Kir4.1* gene-silenced astrocytes. The K^+ influx was not affected by *Kir4.1* shRNA (Fig. 4*E* and *F*). In addition, *Kir4.1* knock down resulted in a partial reduction of astrocytic membrane depolarization (Fig. 4*G* and *H*), when compared with *Trek-1* knockdown (Fig. 3*I* and *J*). We next tested whether voltage-gated potassium channels contribute to the source of an increase in extracellular potassium leading to astrocytic volume change. We measured the IOS change with a general voltage-gated potassium channel inhibitor, 4-AP (4-aminopyridine). We found an increase in IOS amplitude rather than a decrease with 4-AP (Fig. 4*I* and *J*). If any voltage-gated potassium channels were the source of the increase in extracellular potassium, 4-AP would have decreased the IOS signal. However, we observed the opposite result, namely an increase in IOS signal. The increase in IOS signal with 4-AP is most likely due to a prolonged depolarization of the presynaptic terminal and an increased glutamate release, leading to an increase in activation of postsynaptic AMPA and NMDA receptors. This suggests that voltage-gated potassium channels are not the source of the extracellular potassium leading to astrocytic volume change. These results led us to conclude that there is a minimal contribution of NKCC1 and Kir4.1 channels to the K^+ uptake, and voltage-gated potassium channels to the extracellular potassium increase, leading to activity-induced transient volume change.

Volume transient is terminated by Cl^- efflux via BEST1

Next, we explored the molecular identity of the volume decrease following a transient volume increase. In our previous studies, we demonstrated that DCPIB, a specific blocker for VRAC, did not affect the decay of IOS, while NPPB, a general blocker of anion channels, increased the baseline and eliminated the decay of the IOS during repetitive stimulations, suggesting that the volume decrease is mediated by an anion channel, but not by VRAC (Woo *et al.* 2019).

One potential candidate is BEST1, a Ca^{2+}-activated anion channel. BEST1 is highly expressed in hippocampal astrocytes and is dually regulated by Ca^{2+} and volume (Chien & Hartzell, 2007; Spitzner *et al.* 2008; Park *et al.* 2009). To test whether BEST1 is involved in the volume decrease, we utilized BEST1 KO mice (Woo *et al.* 2012) and the cell type specific gene silencing system. In the hippocampus of BEST1 KO mice and *Best1* shRNA

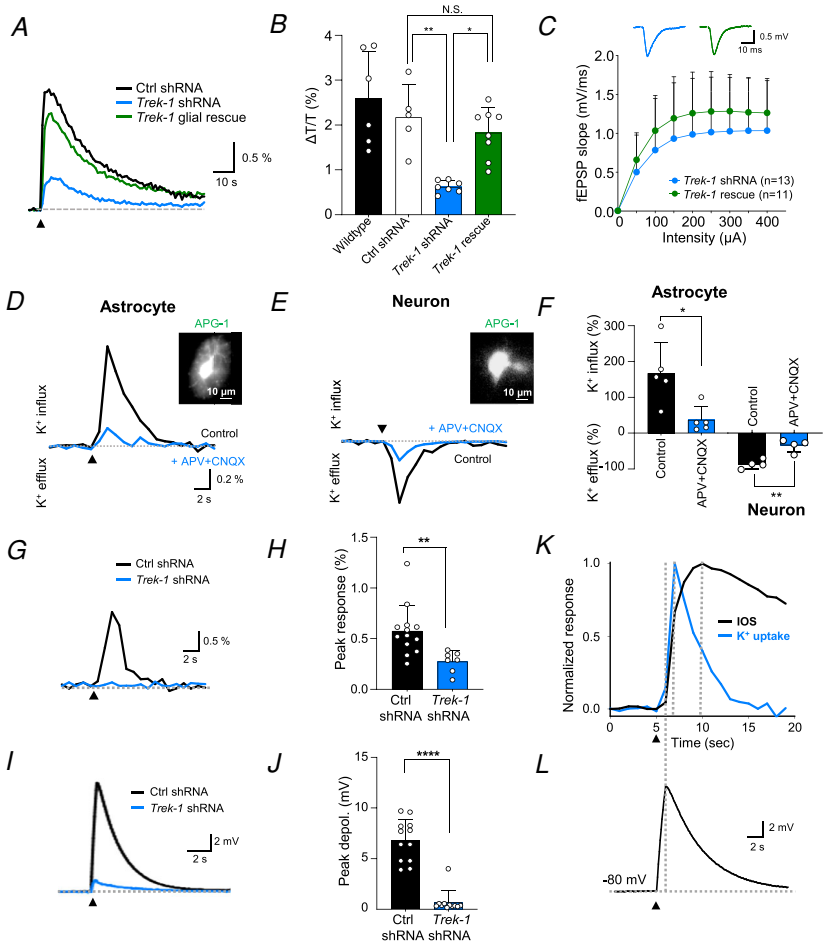

Figure 3. Increase of astrocytic volume transient is mediated by TREK-1 potassium channels
A, representative traces of IOS from hGFAP-CreERT2 mice expressing control shRNA, *Trek-1* shRNA or *Trek-1* shRNA with tamoxifen (*Trek-1* glial rescue). Black triangle: stimulation. *B*, summary bar graph of amplitude of IOS (two-way ANOVA with Bonferroni's *post hoc* multiple comparison test, N.S. $P > 0.05$, $^*P < 0.05$, $^{**}P < 0.01$). *C*, input-output curve of fEPSP amplitude plotted *versus* stimulus intensity (μA). Inset: representative traces of fEPSP at 100 μA stimulation. *P* values were derived from two-way ANOVA with Bonferroni's *post hoc* multiple comparison test. Data values represent means ± S.D. *D* and *E*, measurement of K^+ movement in astrocyte (*D*) and neuron (*E*). Blocking of K^+ influx in astrocyte, and K^+ efflux in neuron, after treatment with APV (50 μM) and CNQX (20 μM). *F*, blocking percentage of K^+ movement by treatment with APV and CNQX (Student's unpaired *t* test $^*P < 0.05$, $^{**}P < 0.01$). *G*, representative traces of K^+ influx in astrocyte from *Trek-1* shRNA or control shRNA-expressing astrocytes. *H*, peak response of K^+ influx (Student's unpaired *t* test, $^{**}P < 0.01$). *I*, representative traces of depolarization in astrocyte from *Trek-1* shRNA or control shRNA-expressing astrocytes. *J*, peak response of depolarization (Student's unpaired *t* test, $^{****}P < 0.0001$). *K*, comparison of timing of K^+ uptake and IOS after normalization by peak response. *L*, simultaneous recording of voltage change in astrocyte. Dotted vertical line indicates peak of each response (voltage change, K^+ uptake and IOS).

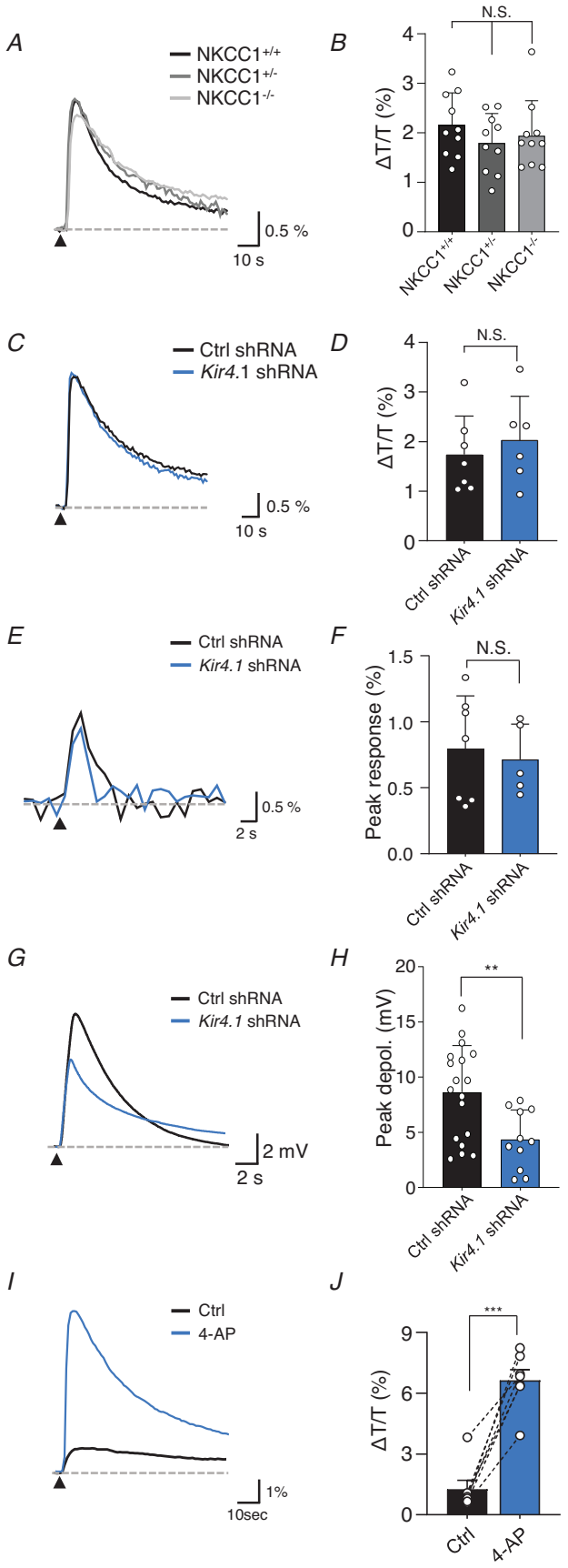

injected mice, we found that the volume decrease was impaired, as evidenced by a raised baseline for the IOS followed by an incomplete decay (Fig. 5*A–C*, *E* and *F* and *H* and *I*). Furthermore, the averaged amplitude of IOS during repetitive stimulations was significantly impaired in the BEST1 KO mice (Fig. 5*G*). However, glial rescue of *Best1* by treating hGFAP-CreERT2 mice with tamoxifen before virus injection fully restored the volume decrease (Fig. 5*D* and *H–J*), suggesting that it is indeed the astrocytic BEST1 that mediates the volume decrease.

To confirm that astrocytic volume decrease requires movement of Cl^- through BEST1, we measured changes in Cl^- concentration in hippocampal astrocytes using a Cl^- sensitive fluorescent dye, MEQ (Sah & Schwartz-Bloom, 1999; Isomura *et al.* 2003). In MEQ-loaded astrocytes, synaptic stimulation induced a fast influx followed by a slow efflux of Cl^- (Fig. 6*A*). The slow efflux of Cl^- was significantly reduced by APV and CNQX (Fig. 6*A* and *B*) and completely eliminated in *Best1* shRNA-expressing astrocytes (Fig. 6*C* and *D*) without affecting the fast influx of Cl^-. By comparing the time courses of Cl^- movement and the IOS, we found that the Cl^- efflux has a time course that is similar to that of the volume decrease (Fig. 6*E*). To determine the source of fast Cl^- influx, we blocked chloride channels by treating with ORG24598, a selective inhibitor of the glial glycine transporter GlyT1 (Brown *et al.* 2001). The fast Cl^- influx was significantly reduced with ORG24598, while slow Cl^- efflux was not changed (Fig. 6*F* and *G*). Therefore, we suggest that Cl^- influx is mediated in part by GlyT1 during volume regulation in astrocyte. These results demonstrate that the synaptic activity-induced volume decrease is mediated by Cl^- efflux via BEST1 in astrocytes.

We next tested a possible candidate member of the VRAC Tweety-homolog (TTYH) family, which we recently reported to encode the pore-forming subunits of the swelling-dependent volume-regulated anion channel

Figure 4. Increase of astrocytic volume transient is independent of NKCC1, Kir4.1 or voltage-gated potassium channels
A, representative IOS trace from *NKCC1* wild littermate, hetero-type, and KO mice. *B*, the average amplitude of IOS in *A* (one-way ANOVA with Tukey's multiple comparison test). N.S. indicates non-significant difference. *C*, representative IOS traces from control and *Kir4.1* shRNA expressing mice. *D*, the average amplitude of IOS in *C* (Student's unpaired *t* test, N.S. $P > 0.05$). *E*, representative traces of K^+ influx in astrocytes expressing *Kir4.1* shRNA or control shRNA. *F*, summary bar graph for peak response of K^+ influx. Data are represented as means ± S.D. (Student's unpaired *t* test, N.S. $P > 0.05$). *G*, representative traces showing membrane depolarization in control and *Kir4.1* shRNA expressing astrocytes. *H*, summary bar graph for peak depolarization in *G* (Student's unpaired *t* test, $^{**}P < 0.01$). *I*, representative IOS traces from control and 4-AP treated brain slice. *J*, the average amplitude of IOS in *I* (Student's paired *t* test, $^{***}P < 0.001$).

($VRAC_{swell}$) in the brain (Han *et al.* 2019), as a target for transient volume decrease. We injected a mixture of viruses carrying the previously confirmed shRNA for *Ttyh1*, *Ttyh2* and *Ttyh3* (Han *et al.* 2019) into hippocampus. We observed no significant difference in IOS baseline change or decay time between *Ttyh 1,2,3* triple gene-silenced condition and control shRNA condition (Fig. 7*A–D*). The averaged amplitude of IOS was also not significantly different between the control and *Ttyh 1,2,3* shRNA injected mice (Fig. 7*E*). These results are consistent with our previous report that the DCPIB-sensitive VRAC is not involved in the transient volume decrease (Woo *et al.* 2019).

TRPA1-mediated Ca^{2+} increase leads to volume decrease

Because BEST1 is a Ca^{2+}-activated anion channel that leads to volume decrease through Cl^- efflux, we hypothesized that a rise in astrocytic Ca^{2+} could lead to a volume decrease. It has been reported that a rise in astrocytic Ca^{2+} can be mediated by either Ca^{2+} release from internal stores through IP_3R2 upon GPCR activation (Agulhon *et al.* 2010) or Ca^{2+} entry via TRPA1 (Shigetomi *et al.* 2011, 2013), which is known to be one of the members of stretch-activated TRP channels (Corey *et al.* 2004; Soya *et al.* 2014). We have recently shown that ultrasound induces a Ca^{2+} increase via TRPA1 and subsequently releases glutamate via BEST1 (Oh *et al.* 2019). Therefore, we tested whether the astrocytic Ca^{2+} increase elicited by the AQP4-dependent volume transient is mediated by TRPA1. Using jRGECO1a (an improved red genetically encoded calcium indicator based on mApple) (Dana *et al.* 2016) under the GFAP104 promoter, we examined the synaptic activity-mediated astrocytic Ca^{2+} response in hippocampal slices. Two consecutive Schaffer collateral stimulations (20 Hz, 1 s), separated by a 15-min interval, induced similar amplitudes of astrocytic Ca^{2+} responses (Fig. 8*A* and *B*). However, the second stimulation-induced Ca^{2+} response was significantly reduced, to 35%, when

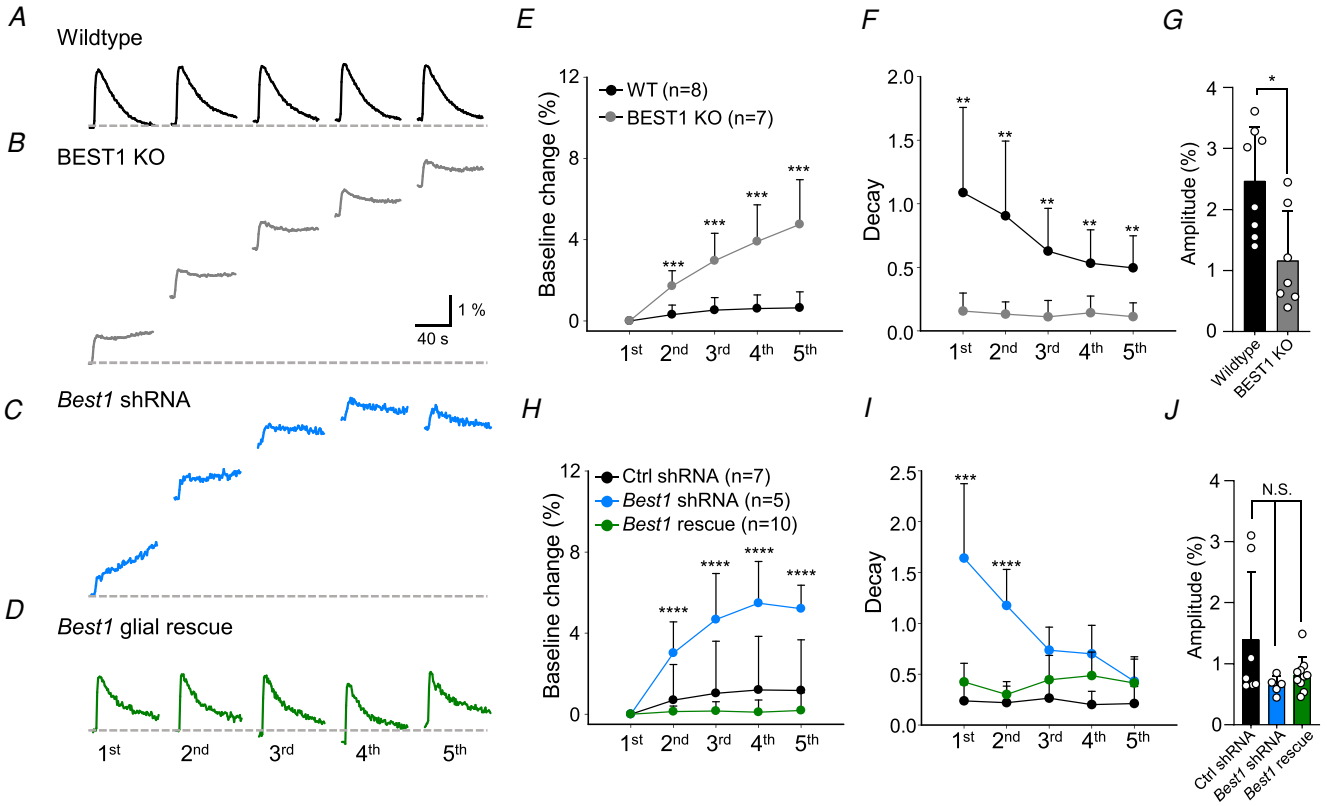

Figure 5. Decrease of astrocytic volume transient is mediated by BEST1 chloride channels
A–D, representative IOS traces from WT, BEST1 KO mice and hGFAP-CreERT2 mice expressing *Best1* shRNA and *Best1* shRNA with tamoxifen (glial rescue of *Best1*). *E* and *F*, summary graphs of baseline (*E*) and decay (*F*) changes of IOS from WT and *Best1* KO mice (multiple *t* test, $^{**}P < 0.01$, $^{***}P < 0.001$). *H* and *I*, summary graphs of baseline (*H*) and decay (*I*) changes of IOS from hGFAP-CreERT2 mice expressing *Best1* shRNA or *Best1* shRNA with tamoxifen (multiple *t* test, $^{***}P < 0.001$, $^{****}P < 0.0001$). *G* and *J*, summary graphs for amplitude of IOS in these conditions. *P* values were derived by Student's *t* test (*G*) and two-way ANOVA with Dunnett's *post hoc* multiple comparison test (*J*). Data are represented means ± S.D. N.S. $P > 0.05$, $^{*}P < 0.05$.

the slice was treated with a selective TRPA1 blocker HC030031 (McNamara *et al.* 2007) for 15 min (Fig. 8*C–E*). These results suggest that the majority of the synaptic activity-induced astrocytic Ca^{2+} increase is induced via TRPA1.

We next used the TRPA1 KO mice and cell-type specific gene-silencing system using *Trpa1* shRNA. In both TRPA1 KO mice and *Trpa1* shRNA injected mice, we found that the volume decrease was impaired, as evidenced by a significantly raised baseline for the IOS followed by an incomplete decay (Fig. 9*A–D*). However, glial rescue of *Trpa1* fully restored the volume decrease (Fig. 9*E–I*). To test whether IP_3R2-dependent Ca^{2+} release is associated with the volume decrease, we measured IOS using IP_3R2 KO mice (Futatsugi *et al.* 2005). We found no significant difference in the IOS baseline or decay (Fig. 10*A–D*). These results suggest that it is indeed TRPA1 that mediates the volume decrease in astrocytes rather than IP_3R2.

Based on our results, we have analysed the time course of IOS signal and ion flows after synaptic activity. The K^+ influx proceeds IOS peak while Cl^- efflux corresponds with IOS decrease (Fig. 11*A*). The Ca^{2+} response that coincides with IOS might be responsible for opening of Ca^{2+}-activated chloride channels (Fig. 11*A*). Taken together, this study provides the detailed molecular and cellular mechanisms of the activity-dependent volume transient in astrocytes (Fig. 11*B*).

Discussion

In the present study, we have provided a new model for the way in which neuronal activity is linked to the astrocytic volume transient (Fig. 11*B*). The whole process begins when an intense neuronal activity causes an opening of postsynaptic AMPA and NMDA receptor channels in neurons that dump out K^+ into the extracellular space (Fig. 11*B*, ①). The volume transient is initiated by an uptake of the extracellular K^+ ions through the TREK-1 containing K2P channels. As a possible counter balancing ion, Cl^- influxes through GlyT1 with the same time course as the K^+ influx through K2P channels (Fig. 11*B*, ②). These ionic fluxes drive the influx of water molecules through the astrocyte-specific AQP4 channel in response to an osmotic pressure, resulting in transient volume increase (Fig. 11*B*, ③). The stretched cell membrane is likely to open TRPA1, to induce a Ca^{2+} influx (Fig. 11*B*,

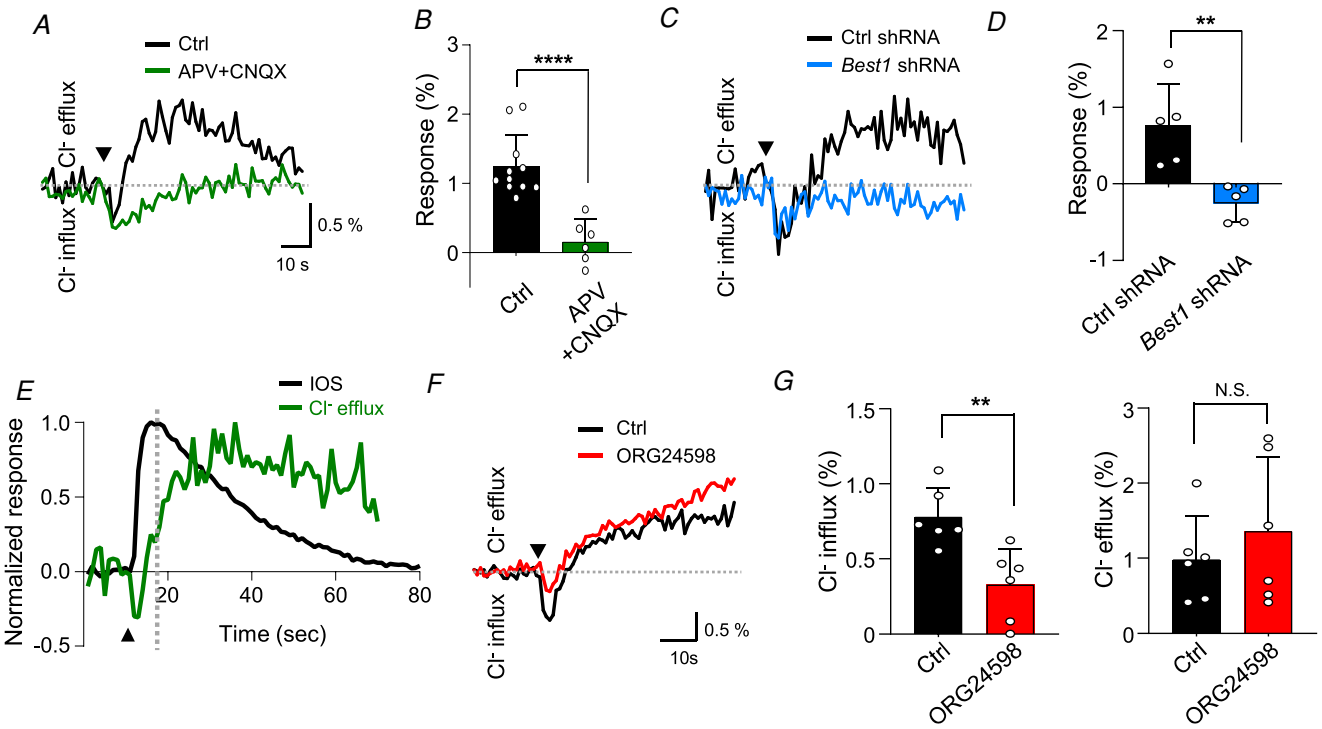

Figure 6. Cl^- efflux during volume transient is mediated by BEST1
A, representative traces of Cl^- efflux in astrocytes from WT mice with or without APV (50 μM) plus CNQX (20 μM) treatment. *B*, magnitude of Cl^- efflux by averaging responses over 50–60 s (Student's unpaired *t* test, $^{***}P < 0.001$). *C*, representative traces of Cl^- efflux in astrocytes expressing *Best1* shRNA or control shRNA. *D*, magnitude of Cl^- efflux by averaging responses over 50–60 s (Student's unpaired *t* test, $^{**}P < 0.01$). *E*, comparison of timing of Cl^- efflux and IOS after normalization by peak response. *F*, representative traces of Cl^- efflux in astrocytes from WT mice with or without ORG24598 (10 μM) treatment. *G*, magnitude of Cl^- influx and efflux by averaging responses over 50–60 s (Student's unpaired *t* test, N.S. $P > 0.05$, $^{**}P < 0.01$).

④). Following this, astrocytic Ca^{2+} can activate BEST1 allowing Cl^- to flow out of astrocyte through this open channel (Fig. 11*B*, ⑤). In response to decreased osmotic pressure, water effluxes through AQP4, resulting in a transient volume decrease (Fig. 11*B*, ⑥).

The molecular identity of the channel responsible for K^+ uptake has long been proposed to be Kir4.1. The astrocytes of the Kir4.1 knockout mouse show an unusually depolarized membrane potential with an impaired K^+ and glutamate uptake (Djukic *et al.* 2007). However, our study demonstrates that Kir4.1 does not mediate volume transient or K^+ uptake, but only affects activity-dependent membrane depolarization (Fig. 4*C–H*). Instead, we found that the TREK-1 containing K2P channel is responsible for K^+ uptake and the volume transient. This TREK-1 containing K2P channel is most likely a heterodimer of TREK-1 and TWIK-1, as we have previously shown (Hwang *et al.* 2014). The discrepancy between the findings using the Kir4.1 knockout mouse and our findings here might have arisen from the fact that the authors (Djukic *et al.* 2007) performed the K^+ uptake experiments at a holding potential of −90 mV under voltage-clamp configuration, which might have selected for an influx of K^+ through

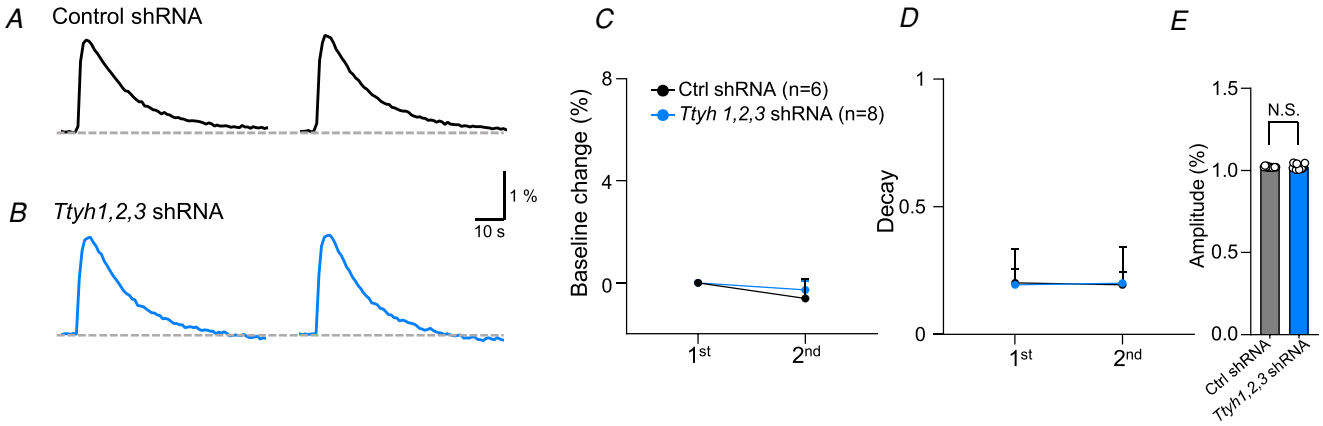

Figure 7. Decrease of astrocytic volume transient is not mediated by TTYH 1,2,3
A and *B*, representative IOS traces from WT mice expressing control shRNA (*A*) and *Ttyh 1,2,3* shRNA (*B*). *C* and *D*, summary graphs of baseline (*C*) and decay (*D*) changes of IOS from control shRNA and *Ttyh 1,2,3* shRNA expressing mice. *E*, summary graph for amplitude of IOS in these conditions. *P* values were derived by Student's unpaired *t* test, N.S. $P > 0.05$.

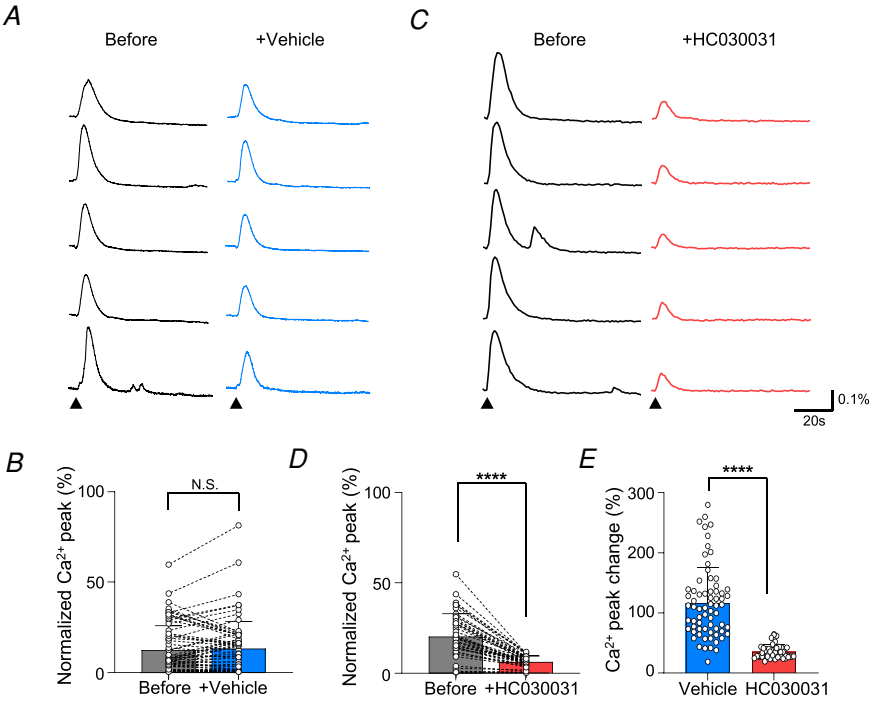

Figure 8. Synaptic activity-induced astrocytic Ca^{2+} increase is mediated via stretch-activated TRPA1 channels
A and *C*, representative Schaffer collateral stimulation-induced Ca^{2+} sensor traces shown before and after vehicle treatment (*A*) and HC030031 (40 μM) treatment (*C*). *B* and *D*, summary graphs of normalized Ca^{2+} peak before and after vehicle treatment (*B*) and HC030031 treatment (*D*) (Student's paired *t* test, N.S. $P > 0.05$, ****$P < 0.0001$). *E*, summary graph of Ca^{2+} peak percentage change in vehicle and HC030031 treated hippocampal slices (Student's paired *t* test, ****$P < 0.0001$).

Kir4.1 (Djukic *et al.* 2007). In other words, the authors might have obtained different results if they had performed the experiment under current-clamp configuration as we did in this study. Therefore, the roles of Kir4.1 and K2P are clearly distinct: Kir4.1 sets up the resting membrane potential whereas K2P mediates passive conductance and K^+ uptake (Pasler *et al.* 2007; Hwang *et al.* 2014).

Likewise, VRAC has long been proposed to be responsible for the transient volume decrease. We have recently reported that astrocytic TTYH1/2/3 are necessary and sufficient for the regulated volume decrease (RVD) in the hippocampus rather than the transient volume decrease (Han *et al.* 2019). RVD is induced by low-frequency stimulation (1 Hz) for 30 min, which is

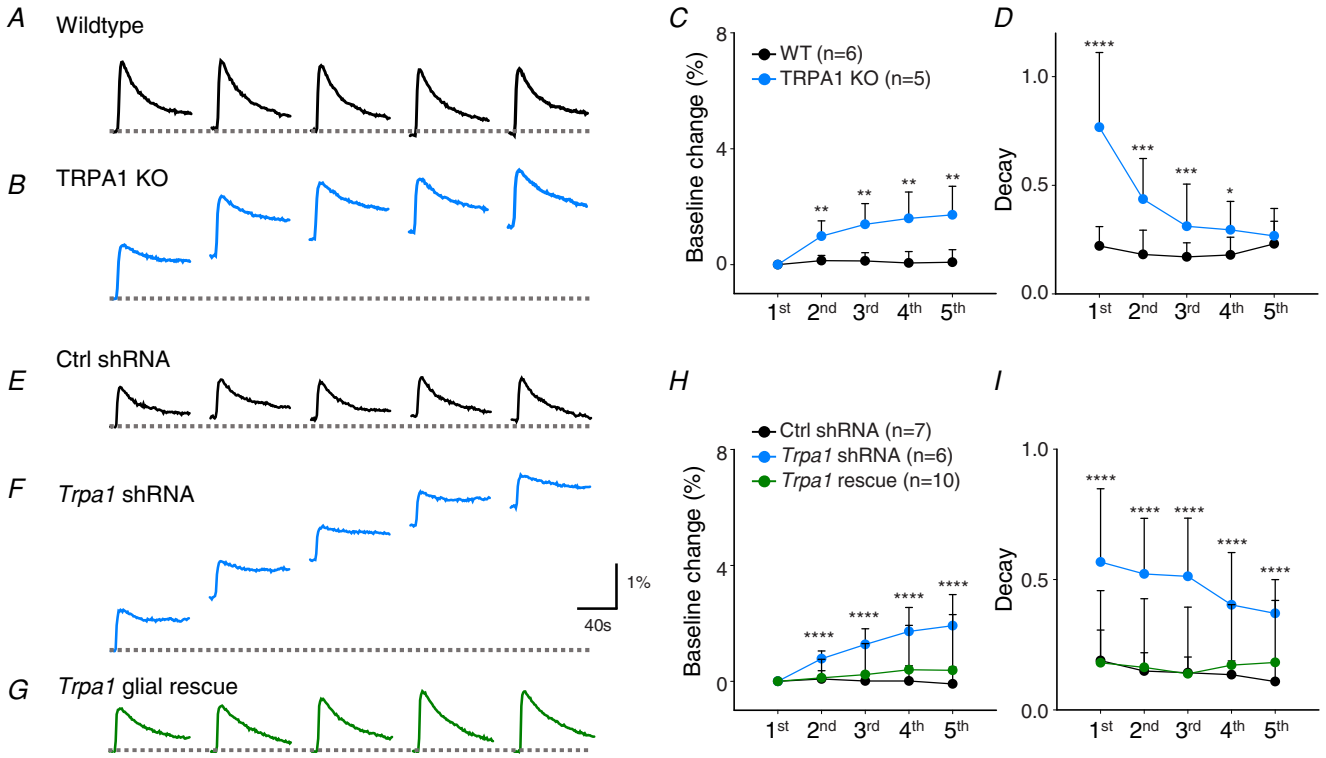

Figure 9. TRPA1-mediated Ca^{2+} increase leads to decrease of volume transient
A and *B*, representative IOS traces from WT and TRPA1 KO mice. *C* and *D*, summary graphs of baseline (*C*) and decay (*D*) changes of IOS from these mice (multiple *t* test, $^*P < 0.05$, $^{**}P < 0.01$, $^{***}P < 0.001$, $^{****}P < 0.0001$). *E-G*, representative IOS traces from hGFAP-CreERT2 mice expressing control shRNA (*E*), *Trpa1* shRNA (*F*), *Trpa1* shRNA with tamoxifen (glial rescue of *Trpa1*) (*G*). *H* and *I*, summary graphs of baseline (*H*) and decay (*I*) changes of IOS from these mice (multiple *t* test, $^{****}P < 0.0001$). Data are represented as means ± S.D.

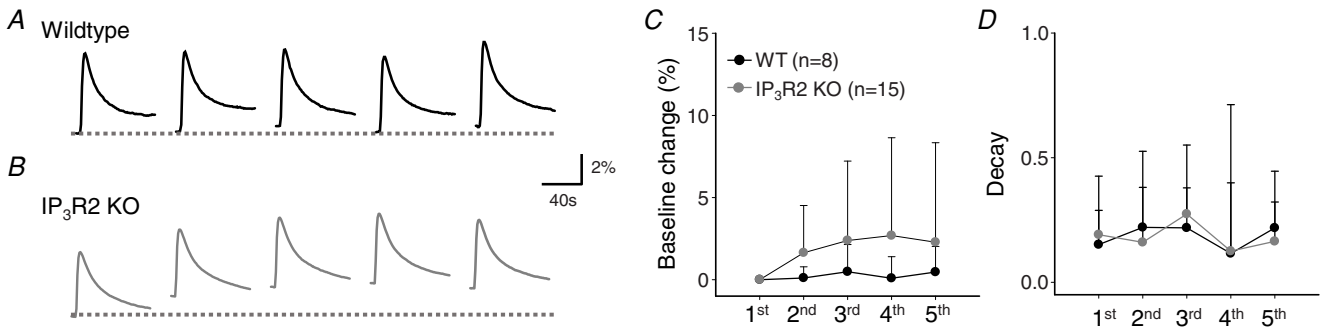

Figure 10. Decrease of astrocytic volume transient is independent of IP_3R2-mediated Ca^{2+} release
A and *B*, representative IOS traces from WT (*A*) and IP_3R2 KO (*B*) mice. *C* and *D*, summary graphs of baseline (*C*) and decay (*D*) changes of IOS from these mice (multiple *t* test, N.S. $P > 0.05$).

clearly distinguishable from the transient volume decrease, which is induced by a brief train of high frequency stimulations. As the TTYH channels have been shown to be responsible for RVD, we expected that these channels would not contribute to the transient volume decrease. As expected, *Ttyh1,2,3* triple gene-silencing did not alter the transient volume decrease. The involvement of LRRC8A in astrocytic volume change has also been indicated using a genetic KO mice model (Yang *et al.* 2019). However, LRRC8A-mediated volume change is also markedly distinct from the transient volume decrease. It is induced by hypo-osmotic solution or ATP treatment,

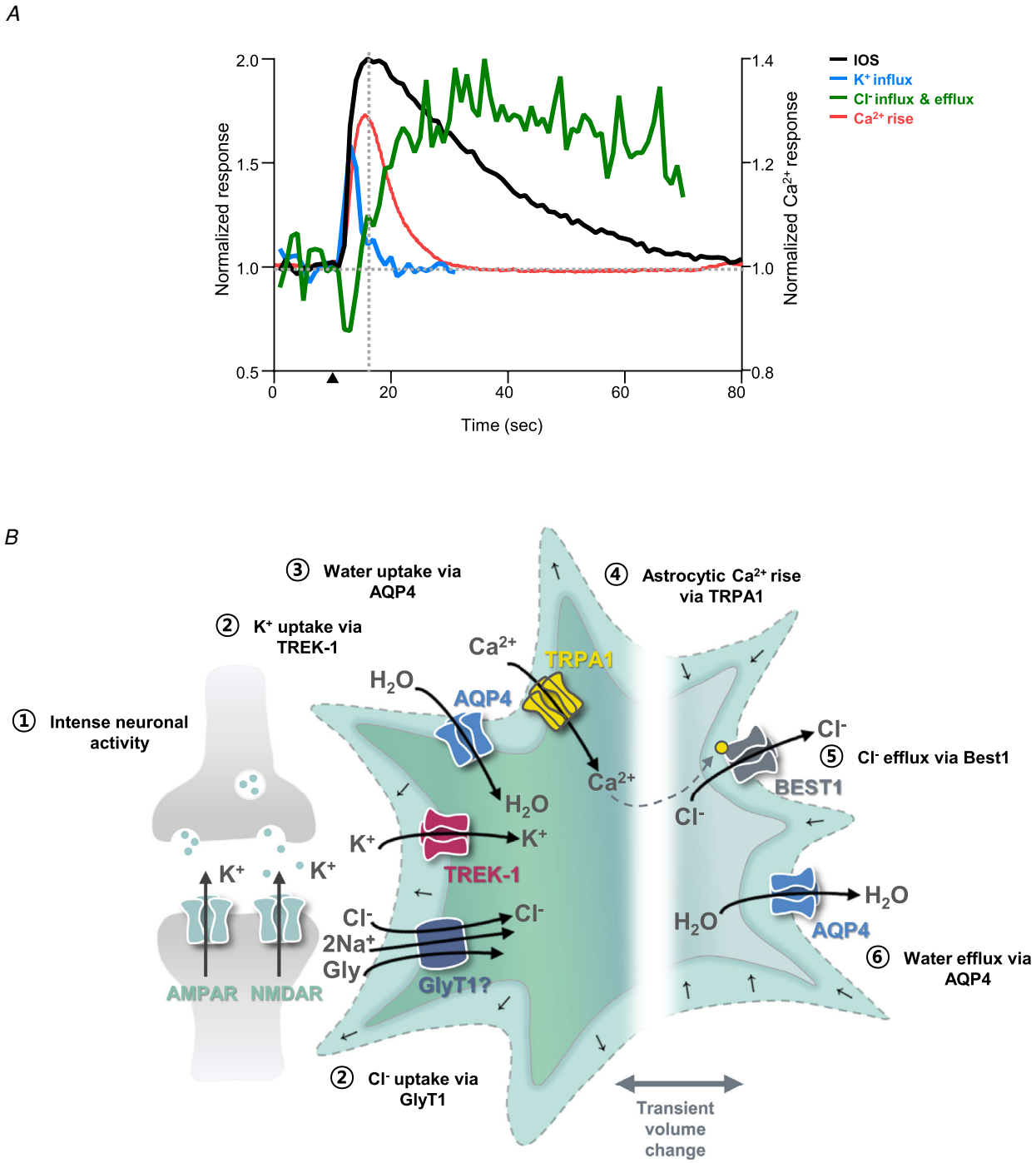

Figure 11. Synaptic activity-induced astrocytic volume transient is time-dependent
A, comparison of timing of IOS, K^+ rise, Cl^- influx and efflux and Ca^{2+} rise. Dotted vertical line indicates the initiation of volume decrease and Cl^- efflux. *B*, schematic diagram depicting molecular mechanism of synaptic activity-induced astrocytic volume increase and decrease.

which cannot be mimicked by a brief train of neuronal activity. In addition, the transient volume decrease has been shown to be insensitive to DCPIB, a specific inhibitor for VRAC (Woo *et al.* 2019). In this study, we have presented a series of results showing that the transient volume decrease is mediated by Cl^- efflux via BEST1. Together, these results all indicate that the transient volume decrease is mediated by Ca^{2+}-activated anion channels such as BEST1, and not by VRACs such as TTYH or LRRC8A.

We have recently shown that astrocytic TRPA1 is modulated by low-intensity, low-frequency ultrasound (LILFU) and mechanical stimulus (poking) to induce an astrocytic Ca^{2+} increase (Oh *et al.* 2019). LILFU can specifically activate TRPA1 in astrocytes, which results in glutamate release through BEST1 (Oh *et al.* 2019). In addition, the similar subcellular localization of TRPA1 and BEST1 in the astrocytic microdomains (Woo *et al.* 2012; Oh *et al.* 2019) provides a structural basis for TRPA1's unique ability to cooperate with the Ca^{2+}-activated BEST1. In the current study, we have additionally demonstrated that astrocytic membrane expansion, induced by a transient volume increase, can activate TRPA1 and subsequently BEST1. These results indicate that an increase in astrocytic Ca^{2+}, which is induced by either ultrasound-activated TRPA1 (Oh *et al.* 2019) or membrane stretch-activated TRPA1, can open BEST1 channels.

Consistent with recent studies describing IP_3R2 independent astrocytic Ca^{2+} signalling in neuronal pathways (Petravicz *et al.* 2014; Srinivasan *et al.* 2015), we also have demonstrated that IP_3R2 is not a major source of the astrocytic Ca^{2+} involved in the synaptic activity-induced volume transient (Fig. 10). We observed in the IP_3R2 KO mouse a tendency of the IOS baseline to generally increase, indicative of some minor involvement of IP_3R2 in the astrocytic Ca^{2+} increase that leads to a transient volume decrease. Nevertheless, the measured values were highly variable, even in slices from the same animal, suggesting that IP_3R2 is not a major contributor to the astrocytic volume transient. In addition to the IOS baseline change, there was also a non-significant difference in the IOS decay in WT and IP_3R2 KO mice, strengthening the argument that transient astrocytic volume change is independent of IP_3R2.

BEST1 has been shown to release glutamate Ca^{2+}-dependently from astrocytes (Oh *et al.* 2012, 2019; Woo *et al.* 2012; Park *et al.* 2013), and the released glutamate targets synaptic GluN2A-containing NMDA receptors to cause NMDAR-dependent potentiation of synaptic activities (Park *et al.* 2015; Oh *et al.* 2019). Activation of AQP4 has also been implicated in synaptic plasticity, in hippocampal volumetric plasticity and long-term potentiation in rodents and grey matter volume increase and verbal learning capacity in humans (Woo *et al.* 2018). AQP4 underlies the overall process of astrocytic transient volume change: a series of sequential events including water influx, transient volume increase, Ca^{2+} increase and subsequent activation of BEST1 during the transient volume decrease.

We observed no change in the fEPSP slope in the *Aqp4* shRNA group (Fig. 2*C*), indicative of intact basal synaptic transmission. On the other hand, previous studies have shown a critical role of AQP4 in LTP and memory without any appreciable differences in basal synaptic transmission (Skucas *et al.* 2011; Fan *et al.* 2013; Woo *et al.* 2018). Consistent with these previous studies, we also anticipate that *Aqp4* genetic knockdown does not disturb neuronal synaptic activity but would result in LTP impairment. We predict that this might be due to a reduction in release of gliotransmitters such as BDNF and/or glutamate in AQP4 lacking astrocytes. Therefore, we raise the possibility that the AQP4-dependent volume transient leads to (1) a TRPA1-mediated Ca^{2+} increase, (2) Ca^{2+}-dependent BDNF and BEST1-mediated glutamate releases, (3) BDNF- and NMDAR-dependent synaptic plasticity and memory formation. These exciting possibilities await future investigations.

In summary, our study identifies several important astrocytic ion channels (AQP4, TREK-1, BEST1, TRPA1) as the key molecules leading to the activity-dependent volume transient in astrocytes. Our study highlights the importance of neuron-astrocyte interaction during an intense synaptic transmission through an unexpected physical phenomenon, the astrocytic volume transient.

References

Abdullaev IF, Rudkouskaya A, Schools GP, Kimelberg HK & Mongin AA (2006). Pharmacological comparison of swelling-activated excitatory amino acid release and Cl^- currents in cultured rat astrocytes. *J Physiol* **572**, 677–689.

Agulhon C, Fiacco TA & McCarthy KD (2010). Hippocampal short- and long-term plasticity are not modulated by astrocyte Ca^{2+} signaling. *Science* **327**, 1250–1254.

Andrew RD, Labron MW, Boehnke SE, Carnduff L & Kirov SA (2007). Physiological evidence that pyramidal neurons lack functional water channels. *Cerebral Cortex* **17**, 787–802.

Araque A, Parpura V, Sanzgiri RP & Haydon PG (1999). Tripartite synapses: glia, the unacknowledged partner. *Trends Neurosci* **22**, 208–215.

Bazargani N & Attwell D (2016). Astrocyte calcium signaling: the third wave. *Nat Neurosci* **19**, 182–189.

Bittner S, Ruck T, Schuhmann MK, Herrmann AM, Maati HM, Bobak N, Gobel K, Langhauser F, Stegner D, Ehling P, Borsotto M, Pape HC, Nieswandt B, Kleinschnitz C, Heurteaux C, Galla HJ, Budde T, Wiendl H & Meuth SG (2013). Endothelial TWIK-related potassium channel-1 (TREK1) regulates immune-cell trafficking into the CNS. *Nat Med* **19**, 1161–1165.

Brown A, Carlyle I, Clark J, Hamilton W, Gibson S, McGarry G, McEachen S, Rae D, Thorna S & Walkerb G (2001). Discovery and SAR of Org 24598 –a selective glycine uptake inhibitor. *Bioorg Med Chem Lett* **11**, 2007–2009.

Cheung G, Sibille J, Zapata J & Rouach N (2015). Activity-dependent plasticity of astroglial potassium and glutamate clearance. *Neural Plast* **2015**, 109–106.

Chien LT & Hartzell HC (2007). Drosophila bestrophin-1 chloride current is dually regulated by calcium and cell volume. *J Gen Physiol* **130**, 513–524.

Corey DP, Garcia-Anoveros J, Holt JR, Kwan KY, Lin SY, Vollrath MA, Amalfitano A, Cheung EL, Derfler BH, Duggan A, Geleoc GS, Gray PA, Hoffman MP, Rehm HL, Tamasauskas D & Zhang DS (2004). TRPA1 is a candidate for the mechanosensitive transduction channel of vertebrate hair cells. *Nature* **432**, 723–730.

Dallerac G, Chever O & Rouach N (2013). How do astrocytes shape synaptic transmission? Insights from electrophysiology. *Front Cell Neurosci* **7**, 159.

Dana H, Mohar B, Sun Y, Narayan S, Gordus A, Hasseman JP, Tsegaye G, Holt GT, Hu A, Walpita D, Patel R, Macklin JJ, Bargmann CI, Ahrens MB, Schreiter ER, Jayaraman V, Looger LL, Svoboda K & Kim DS (2016). Sensitive red protein calcium indicators for imaging neural activity. *Elife* **5**, e12727.

Djukic B, Casper KB, Philpot BD, Chin LS & McCarthy KD (2007). Conditional knock-out of Kir4.1 leads to glial membrane depolarization, inhibition of potassium and glutamate uptake, and enhanced short-term synaptic potentiation. *J Neurosci* **27**, 11354–11365.

Fan Y, Liu M, Wu X, Wang F, Ding J, Chen J & Hu G (2013). Aquaporin-4 promotes memory consolidation in Morris water maze. *Brain Struct Funct* **218**, 39–50.

Futatsugi A, Nakamura T, Yamada MK, Ebisui E, Nakamura K, Uchida K, Kitaguchi T, Takahashi-Iwanaga H, Noda T, Aruga J & Mikoshiba K (2005). IP3 receptor types 2 and 3 mediate exocrine secretion underlying energy metabolism. *Science* **309**, 2232–2234.

Han YE, Kwon J, Won J, An H, Jang MW, Woo J, Lee JS, Park MG, Yoon BE, Lee SE, Hwang EM, Jung JY, Park H, Oh SJ & Lee CJ (2019). Tweety-homolog (Ttyh) family encodes the pore-forming subunits of the swelling-dependent volume-regulated anion channel (VRACswell) in the brain. *Exp Neurobiol* **28**, 183–215.

Holthoff K & Witte OW (1996). Intrinsic optical signals in rat neocortical slices measured with near-infrared dark-field microscopy reveal changes in extracellular space. *J Neurosci* **16**, 2740–2749.

Hwang EM, Kim E, Yarishkin O, Woo DH, Han KS, Park N, Bae Y, Woo J, Kim D, Park M, Lee CJ & Park JY (2014). A disulphide-linked heterodimer of TWIK-1 and TREK-1 mediates passive conductance in astrocytes. *Nat Commun* **5**, 3227.

Isomura Y, Sugimoto M, Fujiwara-Tsukamoto Y, Yamamoto-Muraki S, Yamada J & Fukuda A (2003). Synaptically activated Cl^- accumulation responsible for depolarizing GABAergic responses in mature hippocampal neurons. *J Neurophysiol* **90**, 2752–2756.

Kitaura H, Tsujita M, Huber VJ, Kakita A, Shibuki K, Sakimura K, Kwee IL & Nakada T (2009). Activity-dependent glial swelling is impaired in aquaporin-4 knockout mice. *Neurosci Res* **64**, 208–212.

Lambert IH, Hoffmann EK & Pedersen SF (2008). Cell volume regulation: physiology and pathophysiology. *Acta Physiol (Oxf)* **194**, 255–282.

Lee CJ, Mannaioni G, Yuan H, Woo DH, Gingrich MB & Traynelis SF (2007). Astrocytic control of synaptic NMDA receptors. *J Physiol* **581**, 1057–1081.

Lee S, Yoon BE, Berglund K, Oh SJ, Park H, Shin HS, Augustine GJ & Lee CJ (2010). Channel-mediated tonic GABA release from glia. *Science* **330**, 790–796.

Macaulay N & Zeuthen T (2012). Glial k(+) clearance and cell swelling: key roles for cotransporters and pumps. *Neurochem Res* **37**, 2299–2309.

MacVicar BA, Feighan D, Brown A & Ransom B (2002). Intrinsic optical signals in the rat optic nerve: role for K^+ uptake via NKCC1 and swelling of astrocytes. *Glia* **37**, 114–123.

MacVicar BA & Hochman D (1991). Imaging of synaptically evoked intrinsic optical signals in hippocampal slices. *J Neurosci* **11**, 1458–1469.

McNamara CR, Mandel-Brehm J, Bautista MD, Siemens J, Deranian KL, Zhao M, Hayward NJ, Chong JA, Julius D, Moran MM, & Fanger CM (2007) TRPA1 mediates formalin-induced pain. *Proc Natl Acad Sci U S A* **104**, 13525–13530.

Marmorstein LY, Wu J, McLaughlin P, Yocom J, Karl MO, Neussert R, Wimmers S, Stanton JB, Gregg RG, Strauss O, Peachey NS, & Marmorstein AD (2006). The light peak of the electroretinogram is dependent on voltage-gated calcium channels and antagonized by bestrophin (Best-1). *J Gen Physiol*, **127**(5), 577–589.

Mulligan SJ & MacVicar BA (2006). VRACs CARVe a path for novel mechanisms of communication in the CNS. *Sci STKE* **357**, pe42.

Nagelhus EA & Ottersen OP (2013). Physiological roles of aquaporin-4 in brain. *Physiol Rev* **93**, 1543–1562.

Nam MH, Han KS, Lee J, Won W, Koh W, Bae JY, Woo J, Kim J, Kwong E, Choi TY, Chun H, Lee SE, Kim SB, Park KD, Choi SY, Bae YC & Lee CJ (2019). Activation of astrocytic mu-opioid receptor causes conditioned place preference. *Cell Rep* **28**, 1154–1166.

Oh SJ, Han KS, Park H, Woo DH, Kim HY, Traynelis SF & Lee CJ (2012). Protease activated receptor 1-induced glutamate release in cultured astrocytes is mediated by Bestrophin-1 channel but not by vesicular exocytosis. *Mol Brain* **5**, 38.

Oh SJ, Lee JM, Kim HB, Lee J, Han S, Bae JY, Hong GS, Koh W, Kwon J, Hwang ES, Woo DH, Youn I, Cho IJ, Bae YC, Lee S, Shim JW, Park JH & Lee CJ (2019). Ultrasonic neuromodulation via astrocytic TRPA1. *Curr Biol* **29**, 3386–3401.

Okada Y, Sato K & Numata T (2009). Pathophysiology and puzzles of the volume-sensitive outwardly rectifying anion channel. *J Physiol* **587**, 2141–2149.

Olsen ML & Sontheimer H (2008). Functional implications for Kir4.1 channels in glial biology: from K^+ buffering to cell differentiation. *J Neurochem* **107**, 589–601.

Park H, Han KS, Oh SJ, Jo S, Woo J, Yoon BE & Lee CJ (2013). High glutamate permeability and distal localization of Best1 channel in CA1 hippocampal astrocyte. *Mol Brain* **6**, 54.

Park H, Han KS, Seo J, Lee J, Dravid SM, Woo J, Chun H, Cho S, Bae JY, An H, Koh W, Yoon BE, Berlinguer-Palmini R, Mannaioni G, Traynelis SF, Bae YC, Choi SY & Lee CJ (2015). Channel-mediated astrocytic glutamate modulates hippocampal synaptic plasticity by activating postsynaptic NMDA receptors. *Mol Brain* **8**, 7.

Park H, Oh SJ, Han KS, Woo DH, Park H, Mannaioni G, Traynelis SF & Lee CJ (2009). Bestrophin-1 encodes for the Ca^{2+}-activated anion channel in hippocampal astrocytes. *J Neurosci* **29**, 13063–13073.

Pasler D, Gabriel S & Heinemann U (2007). Two-pore-domain potassium channels contribute to neuronal potassium release and glial potassium buffering in the rat hippocampus. *Brain Res* **1173**, 14–26.

Petravicz J, Boyt KM & McCarthy KD (2014). Astrocyte IP3R2-dependent Ca^{2+} signaling is not a major modulator of neuronal pathways governing behavior. *Front Behav Neurosci* **8**, 384.

Sah R & Schwartz-Bloom RD (1999). Optical imaging reveals elevated intracellular chloride in hippocampal pyramidal neurons after oxidative stress. *J Neurosci* **19**, 9209–9217.

Shigetomi E, Jackson-Weaver O, Huckstepp RT, O'Dell TJ & Khakh BS (2013). TRPA1 channels are regulators of astrocyte basal calcium levels and long-term potentiation via constitutive D-serine release. *J Neurosci* **33**, 10143–10153.

Shigetomi E, Tong X, Kwan KY, Corey DP & Khakh BS (2011). TRPA1 channels regulate astrocyte resting calcium and inhibitory synapse efficacy through GAT-3. *Nat Neurosci* **15**, 70–80.

Simard M & Nedergaard M (2004). The neurobiology of glia in the context of water and ion homeostasis. *Neuroscience* **129**, 877–896.

Skucas VA, Mathews IB, Yang J, Cheng Q, Treister A, Duffy AM, Verkman AS, Hempstead BL, Wood MA, Binder DK & Scharfman HE (2011). Impairment of select forms of spatial memory and neurotrophin-dependent synaptic plasticity by deletion of glial aquaporin-4. *J Neurosci* **31**, 6392–6397.

Soya M, Sato M, Sobhan U, Tsumura M, Ichinohe T, Tazaki M & Shibukawa Y (2014). Plasma membrane stretch activates transient receptor potential vanilloid and ankyrin channels in Merkel cells from hamster buccal mucosa. *Cell Calcium* **55**, 208–218.

Spitzner M, Martins JR, Soria RB, Ousingsawat J, Scheidt K, Schreiber R & Kunzelmann K (2008). Eag1 and Bestrophin 1 are up-regulated in fast-growing colonic cancer cells. *J Biol Chem* **283**, 7421–7428.

Su G, Kintner DB, Flagella M, Shull GE & Sun D (2002). Astrocytes from Na^+-K^+-Cl^- cotransporter-null mice exhibit absence of swelling and decrease in EAA release. *Am J Physiol Cell Physiol* **282**, C1147–C1160.

Srinivasan R, Huang BS, Venugopal S, Johnston AD, Chai H, Zeng H, Golshani P & Khakh BS (2015). Ca^{2+} signaling in astrocytes from Ip3r2$^{-/-}$ mice in brain slices and during startle responses in vivo. *Nat Neurosci* **18**, 708–717.

Szu JI & Binder DK (2016). The role of astrocytic aquaporin-4 in synaptic plasticity and learning and memory. *Front Integr Neurosci* **10**, 8.

Thrane AS, Rappold PM, Fujita T, Torres A, Bekar LK, Takano T, Peng W, Wang F, Rangroo Thrane V, Enger R, Haj-Yasein NN, Skare O, Holen T, Klungland A, Ottersen OP, Nedergaard M & Nagelhus EA (2011). Critical role of aquaporin-4 (AQP4) in astrocytic Ca^{2+} signaling events elicited by cerebral edema. *Proc Natl Acad Sci U S A* **108**, 846–851.

Ventura A, Meissner A, Dillon CP, McManus M, Sharp PA, Van Parijs L, Jaenisch R & Jacks T (2004). Cre-lox-regulated conditional RNA interference from transgenes. *Proc Natl Acad Sci U S A* **101**, 10380–10385.

Verkhratsky A & Kettenmann H (1996). Calcium signalling in glial cells. *Trends Neurosci* **19**, 346–352.

Verkhratsky A, Orkand RK & Kettenmann H (1998). Glial calcium: homeostasis and signaling function. *Physiol Rev* **78**, 99–141.

Woo DH, Han KS, Shim JW, Yoon BE, Kim E, Bae JY, Oh SJ, Hwang EM, Marmorstein AD, Bae YC, Park JY & Lee CJ (2012). TREK-1 and Best1 channels mediate fast and slow glutamate release in astrocytes upon GPCR activation. *Cell* **151**, 25–40.

Woo J, Han YE, Koh W, Won J, Park MG, An H & Lee CJ (2019). Pharmacological dissection of intrinsic optical signal reveals a functional coupling between synaptic activity and astrocytic volume transient. *Exp Neurobiol* **28**, 30–42.

Woo J, Kim JE, Im JJ, Lee J, Jeong HS, Park S, Jung SY, An H, Yoon S, Lim SM, Lee S, Ma J, Shin EY, Han YE, Kim B, Lee EH, Feng L, Chun H, Yoon BE, Kang I, Dager SR, Lyoo IK & Lee CJ (2018). Astrocytic water channel aquaporin-4 modulates brain plasticity in both mice and humans: a potential gliogenetic mechanism underlying language-associated learning. *Mol Psychiatry* **23**, 1021–1030.

Yang J, Vitery MDC, Chen J, Osei-Owusu J, Chu J & Qiu Z (2019). Glutamate-releasing SWELL1 channel in astrocytes modulates synaptic transmission and promotes brain damage in stroke. *Neuron* **102**, 813–827.

Additional information

Data availability statement

The data that support the findings of this study are available from the corresponding author upon reasonable request.

Competing interests

The authors of the manuscript have no conflict of interest.

Author contributions

J.W. and C.J.L. conceived and designed the work; J.W., M.W.J., J.L. and W.K. conducted the acquisition of data; J.W., M.W.J., J.L., W.K. and K.M. performed analysis and interpretation of data for the work; J.W., M.W.J. and C.J.L. drafted the manuscript; J.W., M.W.J., J.L., W.K., K.M. and C.J.L. revised and approved the

final version. All authors have approved the final version of the manuscript and agree to be accountable for all aspects of the work. All persons designated as authors qualify for authorship, and all those who qualify for authorship are listed.

Funding

This study was supported by Institute for Basic Science (IBS), Center for Cognition and Society (IBS-R001-D2) to C.J.L.

Acknowledgments

We thank Dr Min Goo Lee (Yonsei Univ., Seoul, Korea) for supplying *NKCC1* KO mice and Dr Hajime Hirase (RIKEN BSI, Wako, Japan) for arranging and providing the experimental setup in Japan.

Keywords

AQP4, astrocytic volume regulation, BEST1, K2P, TREK-1, TRPA1

Supporting information

Additional supporting information may be found online in the Supporting Information section at the end of the article.

Statistical Summary Document